Korean J. Chem. Eng., **27**(1), 168-173 (2010)
DOI: 10.1007/s11814-009-0337-x

Comparison of catalytic ozonation of phenol by activated carbon and manganese-supported activated carbon prepared from brewing yeast

Guiping Wu*,, Tae-seop Jeong**, Chan-Hee Won**, and Longzhe Cui*,†**

*Key Laboratory of Catalysts and Materials Science of Hubei Province, College of Chemical and Material Science, South-central University for Nationalities, Wuhan 430-074, China
**Department of Environmental Engineering, Chonbuk National University, Jeonbuk 561-756, Korea
(*Received 6 June 2009 • accepted 24 July 2009*)

Abstract−Activated carbon (AC) was prepared using brewing yeast as precursor by chemical activation and manganese was supported on activated carbon (Mn/AC) by adsorption-activation method. The characterizations of prepared AC and Mn/AC and their performance as ozonation catalysts was tested. The results indicated that the crystalline phase of supported manganese was MnO. The total BET surface areas of prepared AC and Mn/AC were found to be 1603.0 m^2/g and 598.9 m^2/g, with total pore volumes of 1.43 and 0.49 cm^3/g, respectively. The average pore diameters of AC and Mn/AC were found to be 3.5 nm and 3.3 nm. Adsorption capacities of phenol onto the produced AC and Mn/AC were determined by batch test, at 25 °C and pH 7. Langmuir and Freundlich isotherm models were used to fit the isotherm experimental data, and the Langmuir isotherm model fitted these two adsorption systems well. The maximum uptakes of phenol by AC and Mn/AC were estimated to be 513.5 mg/g and 128.2 mg/g. The presence of AC prepared from brewing yeast was advantageous for TOC reduction of phenol solution compared with single ozonation, and the greatest TOC removal efficiency was obtained in the presence of Mn/AC. All ozonation reactions followed the pseudo-first-order kinetics model well, the degradation rate of phenol was enhanced in the presence of catalysts, and the more pronounced degradation rate was achieved in O_3/Mn/AC system. The rate constants were determined to be 2.16×10^{-2} min^{-1} for O_3 alone, 5.70×10^{-2} min^{-1} for O_3/AC and 6.82×10^{-2} min^{-1} for O_3/Mn/AC.

Key words: Catalytic Ozonation, Activated Carbon, Manganese, Phenol, Adsorption

INTRODUCTION

Ozone is a powerful oxidant and ozonation processes have been successfully used in water and wastewater treatment [1]. However, ozonation alone has been shown to achieve very limited mineralization of organic compounds in wastewater treatment. It is because of the formation of saturated compounds such as aldehydes, ketones and carboxylic acids. Due to their low reactive nature towards ozone, these compounds tend to accumulate in water [2,3]. To overcome this drawback, the combination of ozone with homogeneous or heterogeneous catalysts in order to activate the decomposition of ozone or improve ozone reaction with several organic compounds has been investigated [4-10] and still is the subject of intense research. Heterogeneous catalytic ozonation, which is one of the most attractive alternatives, aims to enhance removal of more refractory compounds through the transformation of ozone into more reactive species and/or through adsorption and reaction of the pollutants on the surface of the catalyst. Oxides of transition metals, such as manganese [11-14], titanium [4,5] or cobalt [15,16], are amongst the most frequently studied ozonation catalysts. It has been proven by many authors that activated carbon can act initiating the ozone decomposition [1,17-19], leading to the formation of oxygenated active species that are responsible for enhancing the mineralization of organic compounds.

Because a heterogeneous catalytic reaction takes place on the surface of catalysts, the catalytic efficiency of solid catalyst depends greatly on the catalyst and its surface properties, such as surface area and the presence of active sites [20]. Activated carbons, which are produced with carbonaceous materials, have different characters due to different raw materials and activated ways. Brewing yeast, the by-product from the brewing industry, is being produced in large amount annually due to increased volume of beer production [21]. It is generally sold primarily as inexpensive animal feed after inactivation by heat, and much of this by-product is considered industrial organic waste that causes a great deal of concern. Because of the carbonaceous structure and richness in organic materials, yeast is potentially suitable for the production of activated carbon.

Moreover, several authors have mentioned that Mn(II) enhances the activity of ozone. To increase the catalytic activity of activated carbon (AC) and develop the convenient operation of manganese catalyst used in ozonation systems, activated carbon was prepared using brewing yeast as a precursor by chemical activation and manganese was supported on activated carbon (Mn/AC) by adsorption-activation method in present work. Prepared AC and Mn/AC were characterized by nitrogen adsorption at 77 K, X-ray diffraction (XRD) and adsorption experiments. And the performance of AC and Mn/AC as catalysts was tested in the ozonation of phenol in aqueous solution.

MATERIALS AND METHODS

1. Materials

The brewing yeast was collected from King Longquan Beer Com-

†To whom correspondence should be addressed.
E-mail: cuilonger@hotmail.com

pany in Hubei Province of China. The brewing yeast was initially washed thoroughly with water to remove any impurities, dried at 60 °C for 24 h and then ground into powder. The contents of carbon, hydrogen, nitrogen and sulfur were determined by an elemental analyzer (PE24002II, USA) and were found to be 42.3%, 7.4%, 0.6% and 0.08% (w/w), respectively. The ash content was determined by heating the raw material to 650 °C in air atmosphere for 4 h and equaled to 9% by weight. The results indicated that this precursor is suitable for the preparation of activated carbon because of its high carbon content and low ash content.

2. Catalyst Preparation

The AC was prepared by using brewing yeast as a precursor by chemical activation with K_2CO_3 activating agent. The powder of brewing yeast was mixed with K_2CO_3 at a ratio of K_2CO_3/yeast 2 (w/w). The mixture was then placed in a sealed ceramic crucible and kept in a muffle furnace. The temperature was ramped from room temperature to 800 °C and retained for 2 hours in nitrogen atmosphere. After the heating treatment, the carbon was cooled to room temperature, then boiled in 0.1 mol/*l* HCl solution for 20 min and washed by deionized water to remove K_2O. After washing, the carbons were dried at 120 °C and then ground into fine powder for further analysis and characterization.

The manganese supported on activated carbon (Mn/AC) was prepared by the adsorption-activation method. The brewing yeast was impregnated in $Mn(NO_3)_2$ aqueous solution in a shaking incubator at 25 °C for 2 h, then separated and dried at 105 °C. And then, it was treated by the same way of prepared activated carbon to obtain the required Mn/AC catalyst.

3. Textural Characterization of Produced AC and Mn/AC

The textural characterization of the sample was based on the corresponding N_2 equilibrium adsorption-desorption isotherms, determined at 77 K using a Quantachrome Autosorb-1. Prior to the experiment, the sample was outgassed at 200 °C for 6 h. The surface area was obtained by using the BET model for adsorption data in a relative pressure ranging from 0.05 to 0.30. The total pore volume was calculated from the amount of N_2 vapor adsorbed at a relative pressure of 0.99. The pore size distribution was evaluated from the desorption branches of the isotherms by the Barrett-Joyner-Halenda (BJH) method.

4. Analysis of Phenol

The concentration of phenol in the aqueous solution was determined with a spectrophotometer (UV-2450, Shimadzu, Kyoto, Japan) at wavelength 270 nm. Prior to analysis, a technical calibration curve was obtained, and it was very reproducible and linear over the phenol concentration range of 0-50 mg/*l*.

5. Adsorption of Phenol

Adsorption experiments were done to estimate the adsorption capacities of phenol onto produced AC and Mn/AC. Solutions with different initial concentrations of phenol ranging from 50 to 5,000 mg/*l* were prepared. To carry out the adsorption experiments, a constant mass of adsorbent (0.15 g) was weighed into a fifty-milliliter plastic bottle (high-density polyethylene), and 30 ml of phenol solution was added to it. The bottles were sealed and shaken at 160 rpm at a temperature of 25 °C in a shaker. The pH of the solution was adjusted by using either 0.1 mol/*l* HCl or 0.1 mol/*l* NaOH during adsorption experiments. After 4 h, samples of 5 ml were then taken out, separated by centrifugation at 3,000 rpm for 10 min. The solution concentration in the supernatant was determined after an appropriate dilution. The uptake (q_e, mg/g) was calculated from the mass balance, as Eq. (1):

$$q_e = \frac{V_i C_i - V_f C_f}{M} \quad (1)$$

Where V_i and V_f are the initial and final (initial plus added acid or alkali solution) volumes (*l*), respectively. C_i and C_f are the initial and final concentrations (mg/*l*), respectively. M is the mass of adsorbent used (g).

6. Catalytic Ozonation Process

The experimental ozonation system consisted of a tubular glass ozonation reactor (h=400 mm, Φ_{in}=30 mm) equipped with gas inlet and outlet. Phenol aqueous solution (300 ml) and 1.0 g catalyst were added into the reactor. Ozone was produced from air by using an ozone generator (made in Korea). Ozonized air (30×10^{-3} m^3/h, ozone concentration: 0.12 mg/*l*, room temperature and pressure) was continuously bubbled into the solution and flowed upward in the tubular reactor. The excess ozone in the outlet gas was removed by KI solution. Samples were taken at intervals to analyze total organic carbon (TOC) concentrations by a TOC analyzer (Multi N/C 3100, Germany).

RESULTS AND DISCUSSION

1. Characterization of AC and Mn/AC

The crystalline phase of supported Manganese was determined using an X-ray diffractometer (XRD, Bruker D8, Germany) equipped with a graphite monochromated Cu Kα radiation (λ=0.154 nm) operated at 50 mA and 50 kV from 5 to 80°. Fig. 1 displays the X-ray diffraction patterns of Mn/AC. In the Mn/AC sample, the dominant diffraction peaks corresponded to MnO at 2θ of 35.00°, 40.60°, 58.80°, 70.28° and 73.94°, compared with those in the standard powder XRD files (JCPDS) published by the International Center for Diffraction Data.

Since a heterogeneous catalytic reaction takes place on the surface of catalysts, the catalytic efficiency of solid catalyst depends greatly on its surface properties such as surface area and the presence of active sites [20]. The textural characterizations of the AC

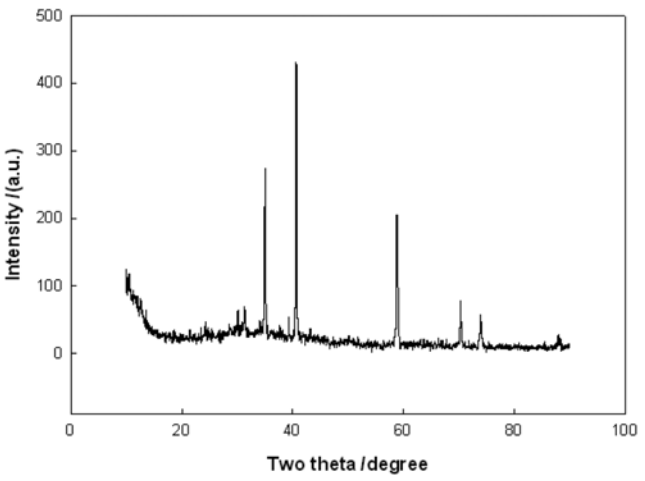

Fig. 1. XRD pattern of Mn/AC.

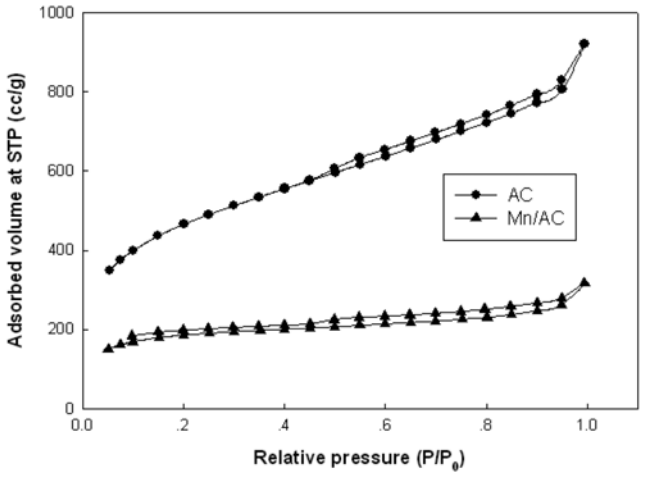

Fig. 2. Adsorption-desorption isotherms of N_2 at 77 K on prepared AC and Mn/AC.

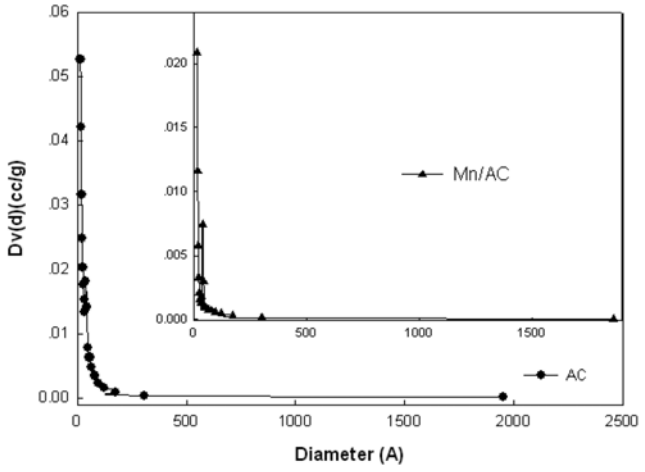

Fig. 3. The pore size distribution of prepared AC and Mn/AC.

and Mn/AC were determined based on the corresponding equilibrium adsorption-desorption isotherms of N_2. Although the BET model has some limitations for the surface area assessment, nitrogen adsorption is still used as a standard procedure for surface area determination, as it can give an accurate assessment of surface area in many types of adsorption isotherms if there is no significant primary micropore filling contribution and the structure of the completed monolayer does not vary from one surface to another. The adsorption-desorption isotherms of N_2 and pore size distribution of prepared AC and Mn/AC are shown in Fig. 2 and Fig. 3, respectively. It was found that the isotherms of AC and Mn/AC exhibited type II character of the BDDT classification. The hysteresis loop in the N_2 adsorption-desorption isotherm indicates the presence of mesopores [22]. The total pore volumes were calculated from the amount of N_2 adsorbed at a relative pressure of 0.99. Table 1 summarizes the surface area and pore volume properties of AC and Mn/AC. The total BET surface areas of prepared AC and Mn/AC were found to be 1,603.0 and 598.9 m^2/g, with total pore volumes of 1.43 and 0.49 cm^3/g, respectively. The average pore diameters of AC and Mn/AC were found to be 3.5 nm and 3.3 nm. Other biomaterials converted into

Table 1. BET surface area, total pore volume and average pore diameter of AC and Mn/AC

Samples	BET surface area (m^2/g)	Total pore volume (cm^3/g)	Average pore diameter (nm)
AC	1063.0	1.43	3.5
Mn/AC	598.9	0.49	3.3

activated carbons include: sugar beet pulp activated with carbon dioxide with surface areas of 200-1,300 m^2/g [23]; bamboo activated with phosphoric acid with surface areas of 697-2,123 m^2/g [22]; palm shell activated with potassium carbonate with surface areas 248-1,170 m^2/g [24]; rice bran activated with sulfuric acid surface areas 200-700 m^2/g [25]. It can be concluded that the surface area and pore volume properties of AC were good and comparable to others activated carbon in the literature [26-28]. Compared to AC, the Mn/AC showed significantly lower BET surface area, pore volume and slightly smaller average pore size. This suggested that part of the manganese species entered into the pore of the support [29].

2. Adsorption of Phenol onto AC and Mn/AC

It is understood that the surface properties of catalyst play an important role in the decomposition of ozone in water into more reactive species. Moreover, when working with organic compounds, it is expected that the adsorption capacity of catalyst towards these compounds also plays a key role during catalytic ozonation processes. On one hand, adsorption competes with the oxidation reaction for the removal of pollutants from the aqueous phase. On the other hand, the adsorption step may play a role in the mechanism of catalytic ozonation. For these reasons, adsorption studies of phenol were done separately on AC and Mn/AC under 25 °C and pH 7, varying the initial phenol concentration within the range 0-5,000 mg/*l*, which resulted in different final concentrations after adsorption equilibrium (4 h) had been achieved. Equilibrium relationships between sorbent and sorbate are usually described by adsorption isotherms, which indicate how the adsorption molecules distribute between the liquid phase and the solid phase when the adsorption process reaches an equilibrium state. The analysis of the isotherm data by fitting them to different isotherm models is an important step to find a suitable model that can be used for design process. The adsorption isotherm is basically important to describe how solutes interact with adsorbents, and is critical in optimizing the use of adsorbents.

Langmuir and Freundlich adsorption isotherms were used to fit the experimental data in this study. The Langmuir isotherm assumes monolayer adsorption onto a surface containing a finite number of adsorption sites of uniform energies of adsorption with no transmigration of adsorbate in the plane of the surface. The linear form of the Langmuir isotherm model is given as Eq. (2):

$$\frac{C_e}{q_e} = \frac{1}{q_m \times b} + \frac{1}{q_m} C_e \quad (2)$$

Where q_e is the amount of phenol adsorbed per unit mass of adsorbent (mg/g), C_e is the equilibrium concentration of the phenol in solution, q_m is the maximum adsorption capacity and b is the constant related to the free energy of adsorption. When C_e/q_e was plotted against C_e, a straight line with slope of $1/q_m$ was obtained, as shown in Fig. 4. The R^2 value (>0.99) indicated that the adsorption data of

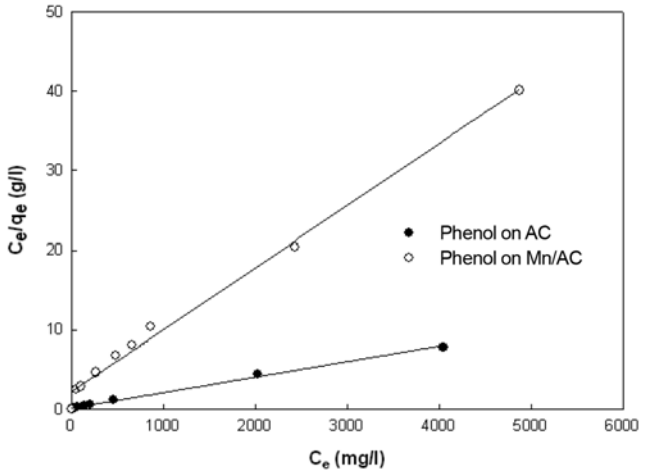

Fig. 4. Langmuir adsorption isotherm of phenol onto AC and Mn/AC at 25 °C and pH 7.

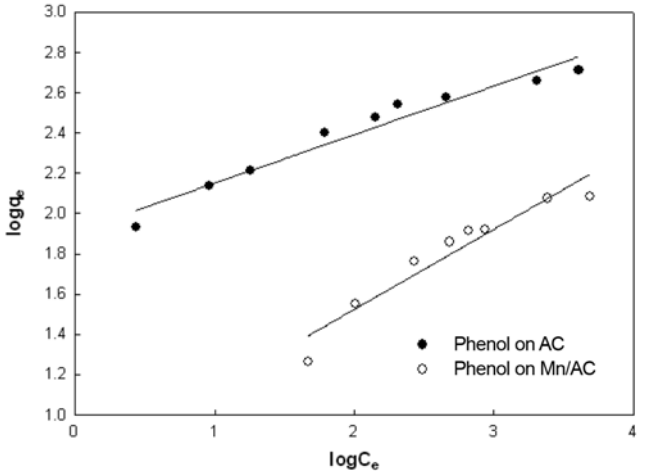

Fig. 5. Freundlich adsorption isotherm of phenol onto AC and Mn/AC at 25 °C and pH 7.

Table 2. Estimated parameters of the Langmuir and Freundlich models

Catalysts	Freundlich model			Langmuir model		
	K_F	n	R^2	q_m (mg/g)	b (1/mg)	R^2
AC	81.30	4.15	0.954	513.5	0.014	0.996
Mn/AC	5.35	2.51	0.920	128.2	0.004	0.993

phenol onto the produced AC and Mn/AC were well fitted to the Langmuir isotherm model. The q_m and constants b were calculated from Eq. (2) and their values listed in Table 2.

Another isotherm model used to fit the experimental data was the Freundlich, which assumes heterogeneous surface energies. The well-known logarithmic form of the Freundlich isotherm is given as Eq. (3):

$$\log q_e = \log K_F + \frac{1}{n}\log C_e \quad (3)$$

Where q_e is the amount of phenol adsorbed per unit mass of adsorbent (mg/g), C_e is the equilibrium concentration of the phenol in solution, K_F and 1/n are empirical constants depending on several environmental factors. K_F can be defined as the adsorption or distribution coefficient and represents the quantity of adsorbate adsorbed onto adsorbent for a unit equilibrium concentration. The slope of 1/n ranging between 0 and 1 is a measure of adsorption intensity or surface heterogeneity, becoming more heterogeneous as its value gets closer to zero [30]. A value for 1/n below one indicates a normal Langmuir isotherm, while 1/n above one is indicative of cooperative adsorption [31]. The plot of $\log q_e$ versus $\log C_e$ gave a straight line, as shown in Fig. 5. The slope of the line was 1/n with value of 0.226 and 0.398 for AC and Mn/AC, indicating a normal Langmuir isotherm. Freundlich constants K_F and n were also calculated and listed in Table 2.

From Table 2, the Langmuir isotherm model yielded better fit with the higher R^2 value compared to the Freundlich model, indicating the homogeneous nature of the AC and Mn/AC derived from brewing yeast in this study. The maximum uptake of phenol by AC and Mn/AC was estimated to be 513.5 mg/g and 128.2 mg/g, respectively. Compared with AC, there is a significant decrease in adsorption capability of Mn/AC. This is in accord with that result of the BET test.

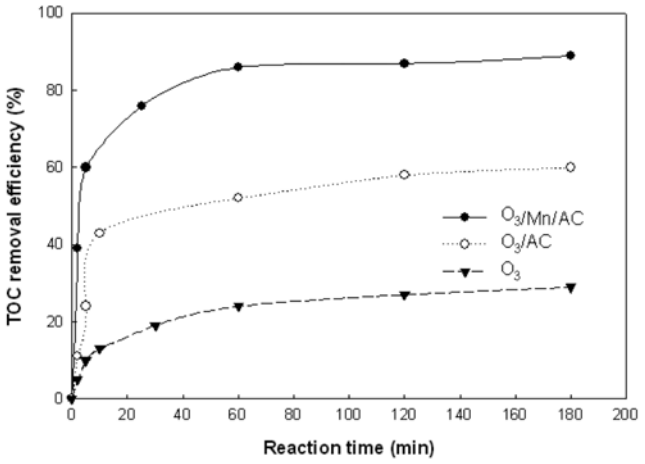

Fig. 6. TOC removal efficiency of phenol in O_3, O_3/AC and O_3/Mn/AC processes.

3. Ozonation of Phenol

To take the effect of adsorption into consideration, the mixture of catalyst and phenol aqueous solution was first stirred for about 60 min without ozone. Then 3.0 ml of mixture was drawn out as the sample of ozonation for 0 min. Other samples were taken at given intervals in the presence of ozone. In this work, the mineralization was checked by measuring the TOC of the solution. The removal efficiency of TOC along with ozonation time under single ozonation (without catalysts) and catalytic ozonation (with AC and Mn/AC) is shown in Fig. 6. It can be seen from Fig. 6 that the presence of AC accelerated the removal of TOC remarkably. For example, in 5 min oxidation time, TOC removal rate for single ozonation was about 10%, that in the presence of AC was 24%. After reaction 10 min, TOC removal rate (43%) in the presence of AC was much greater than that (13%) in only ozonation system. The greater reduction in TOC concentration observed during phenol ozonation in the pres-

ence of AC is largely due to the two roles of AC supposed to play in the catalytic ozonation system. On one hand, it provides a high specific surface area where both organic compounds and ozone can be adsorbed and reacted on it. On the other hand, it promotes the formation of highly oxidant species (•OH), capable of transforming the organic matter into CO_2 [32].

Moreover, the greatest TOC removal rate was obtained in the presence of Mn/AC. After reaction 60 min, TOC removal rate (86%) in the presence of Mn/AC was higher than that (52%) in the presence of AC. This results shows that the catalytic activity of Mn/AC is higher than that of AC. The results of N_2 and phenol adsorption experiments revealed that the adsorption capability of Mn/AC is lower than that of AC. So, the higher activity of Mn/AC is due to MnO, which increases the activity of AC in this phenol ozonation process. These results suggest that manganese is a better active component for the catalytic ozonation of phenol. The adsorption Mn on brewing yeast and chemical activation process support active component Mn and increases its surface active site, which enhances ozone transformation into highly oxidant species (•OH).

4. Kinetics of TOC Removal in Different Processes

The kinetics experiments were performed at initial TOC concentration of around 2,000 mg/L. The results revealed that the removal of TOC can be divided into two-phases, an initial rapid removal phase of TOC (Phase I), followed by a rather slow decomposition phase (phase II). Many researchers have reported this pattern of two-stage kinetics in the decomposition of TCE [33], and pCBA [34] in heterogeneous catalytic ozonation. The data of kinetics experiments were divided into Phase I and Phase II according to reaction rate and were fitted using pseudo-first-order. The linearity plots of $\ln([TOC]_t/[TOC]_0)$ against reaction time are listed in Fig. 7 and the parameters of the pseudo-first-order model are summarized in Table 3. The results show that ozonation alone and catalytic ozonation all followed pseudo-first-order well. As shown in Table 3, the Phase I reaction rate constant was much higher than that of Phase II in these three reaction systems and the removal of TOC was mostly achieved in Phase I. So Phase I reaction is crucial to the efficiency of TOC removal for these three ozonation reaction systems. It can be seen from Fig. 7 that the degradation rate of the single ozonation system was observed

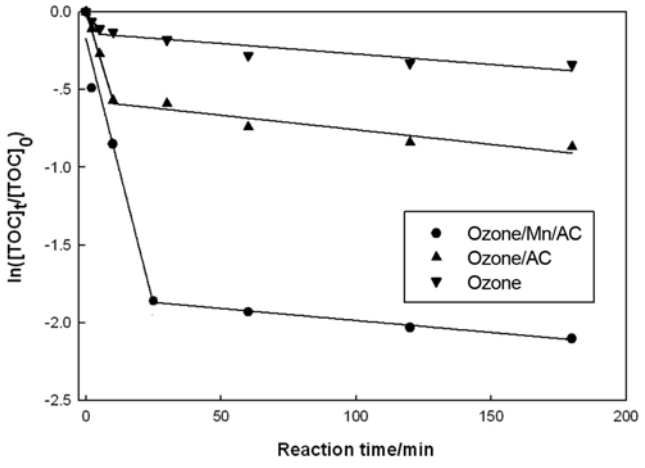

Fig. 7. Pseudo-first-order plot for the degradation of TOC in O_3, O_3/AC and O_3/Mn/AC processes.

Table 3. Pseudo-first-order rate constants of TOC removal in the different systems

Systems	Phase I		Phase II	
	k_1 ($\times 10^{-2}$ min^{-1})	R^2	k_1 ($\times 10^{-2}$ min^{-1})	R^2
Ozone	2.16	0.972	0.13	0.845
Ozone/AC	5.70	0.999	0.19	0.891
Ozone/Mn/AC	6.82	0.966	0.15	0.988

to be lower than that of ozone/AC system, and that of ozone/Mn/AC was the highest in the three processes. The rate constants of Phase I were determined to be 2.16×10^{-2} min^{-1} for O_3 alone, 5.70×10^{-2} min^{-1} for O_3/AC and 6.82×10^{-2} min^{-1} for O_3/Mn/AC, respectively. These observations are consistent with the previous explanation that the presence of AC accelerating the removal of TOC and manganese is a better active component for the catalytic ozonation of phenol.

CONCLUSION

In the present study, activated carbon was prepared using brewing yeast as precursor by chemical activation and manganese was supported on activated carbon (Mn/AC) by adsorption-activation method. The crystalline phase of supported manganese was determined by XRD and found to be MnO. The total BET surface areas of prepared AC and Mn/AC were 1,603 and 598.9 m^2/g, with total pore volumes of 1.43 and 0.49 cm^3/g, respectively. The average pore diameters of AC and Mn/AC were found to be 3.5 nm and 3.3 nm.

Adsorption capacities of phenol onto the produced AC and Mn/AC were determined by batch test, at 25 °C and pH 7. Langmuir and Freundlich isotherm models were used to fit the isotherm experimental data, and the Langmuir isotherm model fitted these two adsorption systems well. The maximum uptakes of phenol by AC and Mn/AC were estimated to be 513.5 mg/g and 128.2 mg/g, respectively.

The presence of activated carbon prepared from brewing yeast was advantageous for TOC reduction compared with single ozonation. Manganese proved to be a better active component for the catalytic ozonation of phenol, and the greatest TOC removal efficiency was obtained in the presence of Mn/AC. After 60 min of reaction, TOC removal rate (86%) in the presence of Mn/AC was greater than that (52%) in the presence of AC and single ozonation (24%).

The results of the kinetic experiments revealed that the removal of TOC can be divided into two-phases, an initial rapid removal phase of TOC (Phase I), followed by a rather slow decomposition phase (phase II). The kinetic reaction data of single ozonation and catalytic ozonation all followed pseudo-first-order well. The Phase I reaction rate constant was much higher than that of Phase II in these three reaction systems, and the removal of TOC was mostly achieved in Phase I. The degradation rate of phenol was enhanced in the presence of catalysts, and the more pronounced degradation rate was achieved in O_3/Mn/AC system. The rate constants Phase I were determined to be 2.16×10^{-2} min^{-1} for O_3 alone, 5.70×10^{-2} min^{-1} for O_3/AC and 6.82×10^{-2} min^{-1} for O_3/Mn/AC.

ACKNOWLEDGMENTS

This work was supported by a grant of Post-Doctoral Program, Chonbuk National University (the First half term of 2008).

REFERENCES

1. P. C. C. Faria, J. J. M. Órfão and M. F. R. Pereira, *Appl. Catal.: Environmental*, **78**, 237 (2008).
2. N. Karpel Vel Leitner, P. Berger and B. Legube, *Environ. Sci. Technol.*, **36**(14), 3083 (2002).
3. M. Skoumal, P.-L. Cabot, F. Centellas, C. Arias, R. M. Rodríguez, J. A. Garrido and E. Brillas. *Appl. Catal. B: Environmental*, **66**, 228 (2006).
4. R. Rosal, A. Rodrguez, M. S. Gonzalo and E. Garca-Calvo, *Appl. Catal. B: Environmental*, **84**, 48 (2008).
5. F. J. Beltrán, F. J. Rivas and R. Montero-de-Espinosa, *Appl. Catal. B: Environmental*, **39**, 221 (2002).
6. J. Rivera-Utrilla and M. Sánchez-Polo, *Appl. Catal. B: Environmental*, **39**, 319 (2002).
7. B. Kasprzyk-Hordern, M. Ziółek and J. Nawrocki, *Appl. Catal. B: Environmental*, **46**, 639 (2003).
8. M. Ernst, F. Lurot and J.-C. Schrotter, *Appl. Catal. B: Environmental*, **47**, 15 (2004).
9. F. J. Beltrán, F. J. Rivas and R. Montero-de-Espinosa, *Appl. Catal. B: Environmental*, **47**, 101 (2004).
10. H. Einaga and S. Futamura, *Appl. Catal. B: Environmental*, **60**, 49 (2005).
11. H. Xiao, R. Liu, X. Zhao and J. Qu, *Journal of Molecular Catalysis A: Chemical*, **286**, 149 (2008).
12. Y. Dong, H. Yang, K. He, S. Song and A. Zhang, *Appl. Catal. B: Environmental*, **85**, 155 (200).
13. L. Zhao, J. Ma, Z. Sun and X. Zhai, *Appl. Catal. B: Environmental*, **83**, 256 (2008).
14. J. Villaseñor, P. Reyes and G. Pecchi, *Catalysis Today*, **76**(2-4), 121 (2002).
15. C.-H. Wu, C.-Y. Kuo and C.-L. Chang, *Journal of Hazardous Materials*, **154**, 748 (2008).
16. P. M. Álvarez, F. J. Beltrán, J. P. Pocostales and F. J. Masa, *Appl. Catal. B: Environmental*, **72**, 322 (2007).
17. H. Valdés and C. A. Zaror, *Chemosphere*, **65**, 1131 (2006).
18. P. C. C. Faria, J. J. M. Órfão and M. F. R. Pereira, *Catalysis Communications*, **9**, 2121 (2008).
19. X. Li, Q. Zhang, L. Tang, P. Lu, F. Sun and L. Li, *Journal of Hazardous Materials*, **163**, 115 (2009).
20. H. Xiong, Y. Zhang, K. Liew and J. Li, *Journal of Molecular Catalysis A: Chemical*, **295**, 68 (2008).
21. W. Lamoolphak, M. Goto, M. Sasaki, M. Suphantharik, C. Muangnapoh, C. Prommuag and A. Shotipruk, *Journal of Hazardous Materials*, **137**, 1643 (2006).
22. A. W. M. Ip, J. P. Barford and G. Mckay, *Bioresour. Technol.*, **99**, 8909 (2008).
23. H. L. Mudoga and H. Yucel, *Bioresour. Technol.*, **99**, 3528 (2008).
24. D. Adinata, W. M. A. Wan Daud and M. K. Aroua, *Bioresour. Technol.*, **98**, 145 (2007).
25. R. M. Suzuki, A. D. Andrade, J. C. Sousa and M. C Rollemberg, *Bioresour. Technol.*, **98**, 1985 (2007).
26. A. T. Mohd Din, B. H. Hameed and A. L. Ahmad, *Journal of Hazardous Materials*, **161**, 1522 (2009).
27. D. J. Kim and J. E. Yie, *J. Colloid Interf. Sci.*, **283**, 311 (2005).
28. Y. Önal, *Journal of Hazardous Materials*, **137**, 1719 (2006).
29. H. Jung, J.-W. Kim, H. Choi, J.-H. Lee and H.-G. Hur, *Appl. Catal. B: Environmental*, **83**, 208 (2008).
30. F. Haghseresht and G. Lu, *Energy Fuels*, **12**, 1100 (1998).
31. K. Fytianos, E. Voudrias and E. Kokkalis, *Chemosphere*, **40**, 3 (2000).
32. L. Zhao, J. Ma, Z. Sun and X. Zhai, *Journal of Hazardous Materials*, **161**, 988 (2009).
33. W.-J. Huang, G.-C. Fang and C.-C. Wang, *Colloids and Surfaces A: Physicochemical and Engineering Aspects*, **260**, 45 (2005).
34. H.-N. Lim, H Choi, T.-M. Hwang and J.-W. Kang, *Water Research*, **36**, 219 (2002).